LA-UR-14-22000

Hydroxide Once or Twice? A Combined Neutron Crystallographic and Quantum Chemical Study of the Hydride Shift in D-Xylose Isomerase

Matt Challacombe* and Nicolas Bock

Theoretical Division, Los Alamos National Laboratory

Paul Langan and Andrey Kovalevsky†

Biology and Soft Matter Division, Oak Ridge National Laboratory

Abstract

We present quantum chemical calculations, through 6-311G**/B3LYP, for the isomerization step in D-Xylose Isomerase, based on truncated models of the 3KCO (linear) and 3KCL (cyclic) X-ray/neutron structures, containing 9 free waters, 2 metals, the sugar and roughly 19 amino acids. Perturbative relaxations upon the experimental framework suggest a possible seven-step mechanism of the isomerzation reaction involving direct ionization of the glucose O2 proton on movement of the mobile magnesium ion (Mg2$A \rightarrow 2B$). In this model, we also find a compensating proton shift between the K183/D255 pair, corresponding to a 10kcal/mol reduction in the cost of the ionization, with a delocalized shift in potential along the reaction plane. We find ∼16 kcal/mol reaction barriers in reasonable agreement with experiment (14 kcal/mol), as well as a final, exothermic hydroxide consistent with the 3CWH (product) structure, and possibly explaining observed non-Michaelis behavior of this enzyme.

Xylose Isomerase (XI) is responsible for aldose to ketose isomerization of hexose and pentose sugars via a hydride shift mechanism [1, 2], and is one of the slowest enzymes known, remaining 5 orders of magnitude slower than triosephosphate isomerase that employs the ene-diol mechanism to catalyze a similar aldose to ketose conversion of triose sugars [3, 4]. Despite its structural elucidation 25 years ago [5], its current industrial relevance [6, 7], and the potential impact on the production of lignocellulosic ethanol [8–11], efforts to improve the activity of XI have yielded results primarily through enhancement of binding and stability [12–15], rather than through acceleration of the catalytic rate k_{cat}.

Perhaps the difficulty in improving catalysis is the complexity and elusive nature of the mechanism, which involves a sugar ring opening step, as well as the isomerization step considered here, taking place in a bridged bimetallic active site that is enclosed in a hydrophobic "shoe-box" [14, 16, 17] that limits solvent exchange when substrate is bound [18]. The active site consists of one metal position responsible for substrate binding, M1, and another with disorder (M2A/B [19] or M2a/b/c [3]) that is thought to initiate the hydride shift on movement, *e.g.* M2A shifts to M2B. High resolution X-ray studies involving Mn and xylitol find the $\text{Mn2}\cdots\text{O}_{\text{cat}}$ distance to be 2.4 Å at Mn2A and 1.8-2.0 Å at Mn2B (2a and 2b/c respectively in Ref. [3]). This result is interpreted as activation of the catalytic water $\text{H}_2\text{O}_{\text{cat}} \rightarrow \text{HO}^-_{\text{cat}}$, which remains in place as M2A shifts to M2B, with hydroxide later serving as the shift initiating base that deprotonates the O2 hydroxyl of the linear glucose [3, 20–23]. In this interpretation, the hydroxide ion is generated twice,

*matt.challacombe@freeon.org
†kovalevskyay@ornl.gov

first in order to abstract the proton from O2 of glucose (ostensibly involving an intermediate base such as D257 [3]), and again after the hydride shift, following the protonation of fructose O1. Offering a counterexample however, the recent joint X-ray/neutron structure of XI in complex with linear D-glucose (PDB ID 3KCO) [19] reveals the catalytic water with both M2B$\cdots$O$_{\rm cat}$ = 2.0Å and M2A$\cdots$O$_{\rm cat}$ = 2.7Å, suggesting that the observed difference in bond lengths does not necessarily correspond to a change in ionization. Also, extended theoretical studies and crystallographic surveys by the Glusker lab demonstrate that a Mg$\cdots$O bondlength of ∼2.0Å is consistent with octahedral coordination of Mg^{2+} [24]. Finally, the "hydroxide twice" scheme leaves the close contact D287-O$\delta2^-\cdots$O2$^-$-glucose unshielded, moreso when including the hydride shift and M2B shifts to M2A. Here we consider an alternative "hydroxide once" mechanism that does not involve an intermediate base; instead the glucose-O2H proton is ionized directly by the M2A-to-M2B movement as suggested by Collyer & Blow [25, 26], with D287-O$\delta2^-$ accepting the initiating proton as argued by Fenn, Ringe & Petsko [3].

Previous theoretical work on XI has been based on X-ray data, without knowledge of proton locations, with severely truncated quantum regions (*i.e.* ommitting shoe box rings), and also based on many-parameter semi-empirical and QM/MM models [22, 32, 33]. In this work, we employ only the *ab initio* B3LYP/6-31G** and B3LYP/6-311G** chemistries [34, 35], and only the Mg substituted 3KCO structure, developing a 306 atom charge neutral model of the active site through constrained geometry optimization as described in the Supporting Information (**I**, Fig. 1A and Fig. 6B). On optimization, the rigorous M1 and M2A octahedral coordination maintained in the crystal structure by Ni relax, with Mg1 moving slightly by 0.2Å and Mg2A moving 0.3Å. Different than the 3KCO structure, the H54-NζH$^+$ proton is transferred to glucose-O5, and the catalytic water (colored in purple) shifts to establish a closer three-fold coordination with O$\delta2$ of D257, O1 of glucose and Mg2A as shown in Fig. 1A and Fig. 6B (Supporting Information), corresponding to a shortening of the Mg2A$\cdots$O$_{\rm cat}$ distance from 2.7Å to 2.0Å.

Starting from **I** (Fig. 1A and Fig. 6B), optimization with internal coordinate constraints [27] was used to probe local minima corresponding to simple chemical transformations corresponding to deprotonation of glucose O2H as Mg2A shifts to Mg2B (ionization) [25, 26], with D287-O$\delta2$ accepting the proton. This first step is supported by recent work, showing that the D287N mutant inactivates XI [15]. The reaction path for this transformation is shown in Fig. 1, with Mg2 moving roughly in a plane defined by O1,O2, C1 & C2 of glucose, and the computed Mg1$\cdots$Mg2 distance changing from 5.0 to 3.5 Å and glucose-O2$\cdots$HO$\delta2$-D287 tending to 2.5 Å. Also shown in Fig. 1B&C, a proton is shifted 0.6 Å from K183 to D255, yielding the K183-H$_2$N$\zeta\cdots$HO$\delta2$-D255 uncharged pair. We re-optimized structure **III** in Fig. 1C with the proton constrained to Nζ of K183, revealing an energetic cost of ∼10kcal/mol (Fig.4) and a delocalized change in the electrostatic potential, shown in Fig. 1C as ±0.2 au orange and purple isosurfaces. Part of this change in potential is oriented along the O1$\cdots$O2 axis, whilst the other part is localized on D255 (and K183, not shown), roughly transverse and alternating with respect to the aforementioned plane. This charge compensation is supported by previous mutagenesis studies: For example, the negative impact on $k_{\rm cat}$ with G219F and G219N mutations [14] may be due to steric interference. Also, the inactivating mutations K183S, K183Q, K183R either remove or dramatically reduce the side-chain's ability to donate a proton to D255[16].

In our model, the hydride shift is accompanied by the shift of Mg2B to Mg2A, shown in Fig. 2. Consistent with the a, b & c des-

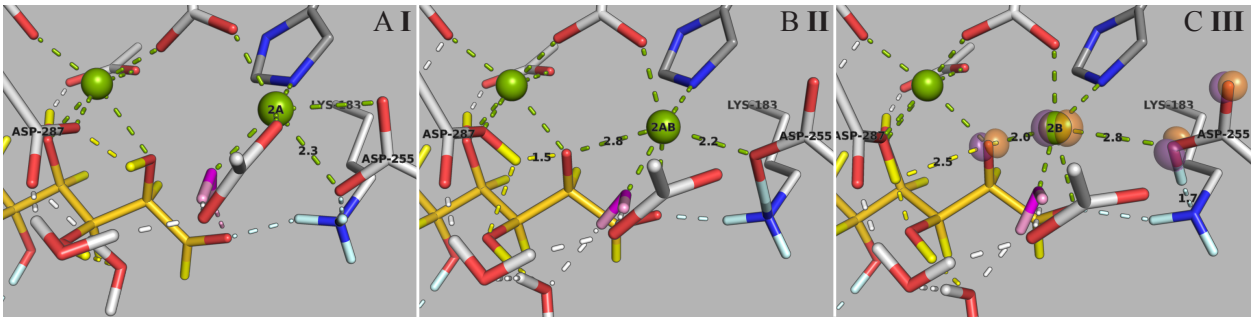

FIG. 1. Mg2A shifts to Mg2B, ionizing the glucose-O2 hydroxyl with the proton (yellow) leaving to D287-Oδ2 (A&B, structures **I**&**II**). Concomitantly, a proton is transferred from K183-NζH$_3^+$ to D255-Oδ2$^-$ (pale blue, B&C, structures **II**&**III**).

ignation of Fenn, Ringe & Petsko [3] for the transient positions of Mg2, the reaction path for the hydride shift is "L" shaped, with Mg2 moving first towards D255 as the hydride shift occurs, Fig. 1A&B, then towards D257 as O1 abstracts a proton from the catalytic water, Fig. 2B&C. Consistent with Allen *et al.*'s [28] structure of the putative transition state analogue D-threonohydroxamic acid (THA) complexed with XI, we also find a Mg1$\cdots$Mg2 distance of 4.1 Å at the transition state, **IV** in Fig. 2B. The computed hydroxide intermediate (**V**) is also supported by the 3CWH structure, in which linear D-xylulose and hydroxide are observed [29] with a 2.2Å Mg2A$\cdots$O$_{\rm cat}$H$^-$ bondlength *vs.* 2.0 computed; **V** was obtained independently from 3CWH, through optimization of **I** involving simple constraints on Mg2 and the initiating proton.

Finally, the catalytic water is regenerated through the Grotthuß mechanism mediated by O3 hydroxyl of glucose and a nearby water, bridging D287-Oδ2H and catalytic hydroxide as shown in Fig. 3, with a substantial enthalpy drop of approximately -20 kcal/mol. It is worth noting the energetically shallow plateau that characterizes the intermediate structure **V** that contains the hydroxide and product fructose (Fig. 4), and that a reaction coordinate with energetics similar to the path **V**$\rightarrow$**VII** branches to regenerate the catalytic water with K183-NζH$_3^+$ donating a proton to O1 of fructose as in Ref. 22, but leaving the active site with widely separated ionization states to be resolved by solvent exchange; an event unlikely to resolve due to the shielded nature of the active site with bound substrate [18].

Shown in Fig.4, our energetic results have three features consistent with observation: First, we find enthalpic activation barriers of $\sim$16 kcal/mol, in reasonable agreement with experiment (14 kcal/mol [1]). Second, the large enthalpic drop on isomerization is exothermic, consistent with non-Michaelis kinetics [25, 26] and observation of the hydroxide intermediate [29] (corresponding to structure **V**). Third, kinetic isotope effect measurements utilizing deuterium-labeled substrates or D2O suggest a partial rate limiting behavior between two steps: (1) a pH sensitive step commensurate with exchange between water and a substrate hydroxyl proton and (2) the hydride shift [2]. The partial limiting behavior of these two steps is consistent with the proposed mechanism as well as the two equi-enthalpic peaks corresponding to structures **II** and **IV**.

In the proposed mechanism, mechanistically diagrammed in Fig. 7, the steps deriving from our initial structure are indirectly confirmed, yet **I** is notably in tension with the M2A occupation of the 3KCO structure (Fig. 6A), as well as others [3], involving a weak 2.7-2.4Å M2A$\cdots$O$_{\rm cat}$ contact, while we

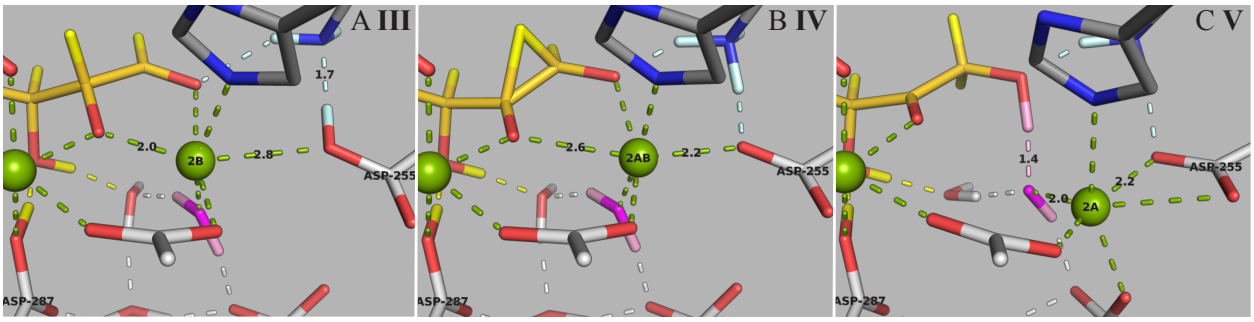

FIG. 2. Mg2B shifts to Mg2A, concurrent with the hydride shift (A&B, structures **III**&**IV**). Hydroxide is formed by abstraction of a proton from the catalytic water (pink) by O1 (B&C, structures **IV**&**V**).

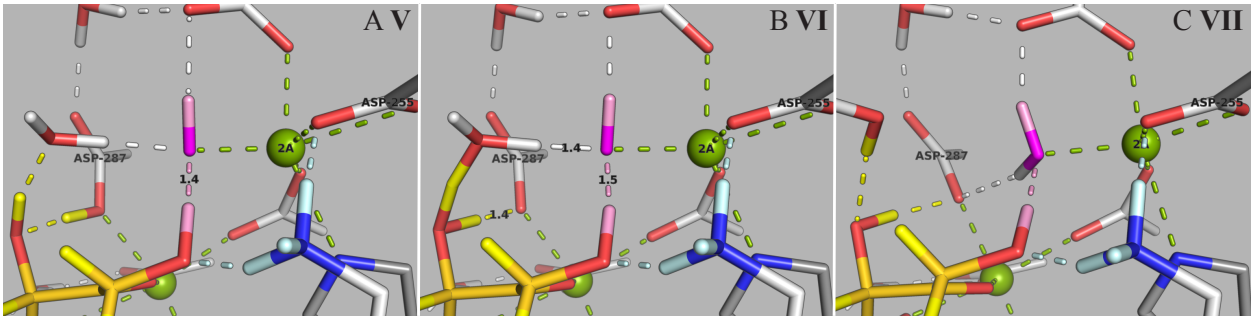

FIG. 3. The ionized proton (D287-Oδ2H, yellow) is reconciled with the catalytic hydroxide (pink) through proton hopping involving glucose-O3 and HOH1105 (A&B, structures **IV**&**V**), followed by exothermic regeneration of the catalytic water to yield four-fold coordination (C&D, structures **V**&**VI**). Compare with, *e.g.* threefold coordination in Fig. 1A.

find a 2.0Å bondlength consistent with other work [24, 29, 30]. Perhaps resolving this tension, close examination of the difference FO-FC electron density maps in several ultra-high resolution X-ray structures hint at multiple positions for H_2O_{cat} [3, 4, 31]. In either case, Fig. 6A or 6B, an initial state appears to involve a catalytic water with three primary contacts, while the product state may include an additional contact corresponding to an exothermic drop and possibly explaining the non-Michaelis behavior of XI.

ACKNOWLEDGMENTS

This work was supported by the U. S. Department of Energy under Contract No. DE-AC52-06NA25396 and LDRD-ER grant 20120256ER.

[1] Allen, K.N., Lavie, A., Farber, G.K., Glasfeld, A., Petsko, G.A., and Ringe, D. (1994) *Biochemistry*, **33** (6), 1481–7.

[2] Bastelaere, P.V. (1995) *Biochem. J*, **307** Pt 1, 135–42.

[3] Fenn, T.D., Ringe, D., and Petsko, G.A. (2004) *Biochemistry*, **43** (21), 6464–74.

[4] Toteva, M.M., Silvaggi, N.R., Allen, K.N., and Richard, J.P. (2011) *Biochemistry*, **50** (46), 10 170–81.

[5] Henrick, K., Collyer, C.A. and Blow D.M. (1989) *Biochemistry*, **50** (46), 10 170–81. *J*

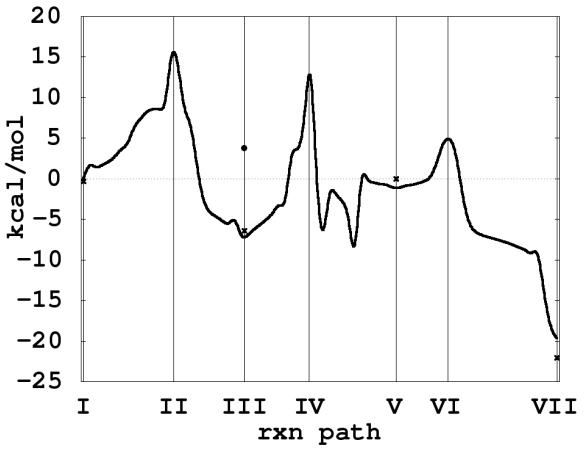

FIG. 4. Reaction path for the putative "hydroxide once" mechanism at the B3LYP/6-31G** level of theory, with larger B3LYP/6-311G** calculations at labeled minima marked by ×s. Also shown (•) is the energy difference for structure **III** with the K183-$H_2N\zeta\cdots H$ bondlength constrained back to its original 0.98Å, corresponding to the isosurfaces shown in Fig. 1C.

Mol Biol. **208** (1):129–57.

[6] Bhosale, S.H., Rao, M.B., and Deshpande, V.V. (1996) *Microbiol. Rev.*, **60** (2), 280–300.

[7] Hahn-Hägerdal, B., Karhumaa, K., Fonseca, C., Spencer-Martins, I., and Gorwa-Grauslund, M.F. (2007) *Appl. Microbiol. Biotechnol.*, **74** (5), 937–53.

[8] van Maris, A.J.A., Winkler, A.A., Kuyper, M., de Laat, W.T.A.M., van Dijken, J.P., and Pronk, J.T. (2007) *Adv. Biochem. Eng. Biotechnol.*, **108**, 179–204.

[9] Wisselink, H.W., Toirkens, M.J., Wu, Q., Pronk, J.T., and van Maris, A.J.A. (2009) *Appl. Environ. Microbiol.*, **75** (4), 907–14.

[10] Young, E., Lee, S.M., and Alper, H. (2010) *Biotechnol. Biofuels*, **3**, 24.

[11] Tomás-Pejó, E., Ballesteros, M., Oliva, J.M., and Olsson, L. (2010) *J. Ind. Microbiol. Biotechnol.*, **37** (11), 1211–20.

[12] Lee, S.M., Jellison, T., and Alper, H.S. (2012) *Appl. Environ. Microbiol.*, **78** (16), 5708–16.

[13] Hlima, H.B., Aghajari, N., Ali, M.B., Haser, R., and Bejar, S. (2012) *J. Ind. Microbiol. Biotechnol.*, **39** (4), 537–46.

[14] Hlima, B.H., Bejar, S., Riguet, J., Haser, R., and Aghajari, N. (2013) *Appl. Microbiol. Biotechnol.*, online, doi:10.1007/s00253-013-4784-2.

[15] Waltman, M.J., Yang, Z.K., Langan, P., Graham, D.E., and Kovalevsky, A. (2014) *Protein Eng. Des. Sel.*, **27** (2), 59–64.

[16] Lambeir, a.M., Lauwereys, M., Stanssens, P., Mrabet, N.T., Snauwaert, J., van Tilbeurgh, H., Matthyssens, G., Lasters, I., De Maeyer, M., and Wodak, S.J. (1992) *Biochemistry*, **31** (24), 5459–66.

[17] Katz, A.K., Li, X., Carrell, H.L., Hanson, B.L., Langan, P., Coates, L., Schoenborn, B.P., Glusker, J.P., and Bunick, G.J. (2006) *Proc. Natl. Acad. Sci. U. S. A.*, **103** (22), 8342–7.

[18] Rose, I.A., O'Connell, E.L., and Mortlock, R.P. (1969) *Biochim. Biophys. Acta*, **178** (2), 376–9,

[19] Kovalevsky, A.Y., Hanson, L., Fisher, S.Z., Mustyakimov, M., Mason, S.a., Forsyth, V.T., Blakeley, M.P., Keen, D.a., Wagner, T., Carrell, H.L., Katz, A.K., Glusker, J.P., and Langan, P. (2010) *Structure*, **18** (6), 688–99.

[20] Whitlow, M., Howard, A.J., Finzel, B.C., Poulos, T.L., Winborne, E., and Gilliland, G.L. (1991) *Proteins*, **9** (3), 153–73.

[21] Lavie, A., Allen, K.N., Petsko, G.A., and Ringe, D. (1994) *Biochemistry*, **33** (18), 5469–5480.

[22] Hu, H., Liu, H., and Shi, Y. (1997) *Proteins*, **27** (4), 545–55.

[23] Garcia-Viloca, M., Alhambra, C., Truhlar, D.G., and Gao, J. (2003) *J. Comput. Chem.*, **24** (2), 177–90.

[24] Markham, G., Glusker, J., and Bock, C. (2002) *J. Phys. . . .*, **106** (19), 5118–5134.

[25] Collyer, C.a. and Blow, D.M. (1990) *Proc. Natl. Acad. Sci. U. S. A.*, **87** (4), 1362–6.

[26] D. M. Blow, P. Brick, C. A. Collyer, J.D.G. and Smart, O. (1992) *Philos. Trans. Phys.*

Sci. Eng., **340** (1657), 311–321.

[27] Németh, K. and Challacombe, M. (2004) *J. Chem. Phys.*, **121** (7), 2877–2885.

[28] Allen, K.N., Lavie, A., Petsko, G.A., and Ringe, D. (1995) *Biochemistry*, **34** (11), 3742–9.

[29] Kovalevsky, A.Y., Katz, A.K., Carrell, H.L., Hanson, L., Mustyakimov, M., Fisher, S.Z., Coates, L., Schoenborn, B.P., Bunick, G.J., Glusker, J.P., and Langan, P. (2008) *Biochemistry*, **47** (29), 7595–7.

[30] Rutkowska-Zbik, D., Witko, M., and Fiedor, L. (2013) *J. Mol. Model.*, **19** (11), 4661–7.

[31] Fenn, T.D.; Ringe, D.; Petsko, G. (2002) *Tech. Rep.*, PDB ID 1MUW, Personal communication.

[32] Asbóth, B. and Náray-Szabó, G. (2000) *Curr. Protein Pept. Sci.*, **1** (3), 237–54.

[33] Garcia-Viloca, M., Alhambra, C., Truhlar, D.G., and Gao, J. (2002) *J. Am. Chem. Soc.*, **124** (25), 7268–9.

[34] Becke, A. (1993), *J. Chem. Phys.*, **98**, 5648

[35] Becke, A. (2014), *J. Chem. Phys.*, **140**, 18A301

[36] Bock, N., Challacombe, M., Gan, C.K., Henkelman, G., Nemeth, K., Niklasson, A., Odell, A., Schwegler, E., Tymczak, C.J., and Weber, V. (2014), FreeON:. URL `freeon.org`.

[37] Henkelman, G., Uberuaga, B.P., and Jonsson, H. (2000) *J. Chem. Phys.*, **113** (22), 9901.

I. SUPPORTING INFORMATION

Hydroxide Once or Twice? A Combined Neutron and Quantum Study of the Hydride Shift in Xylose Isomerase

Matt Challacombe, Nick Bock, Paul Langan and Andrey Kovalevsky

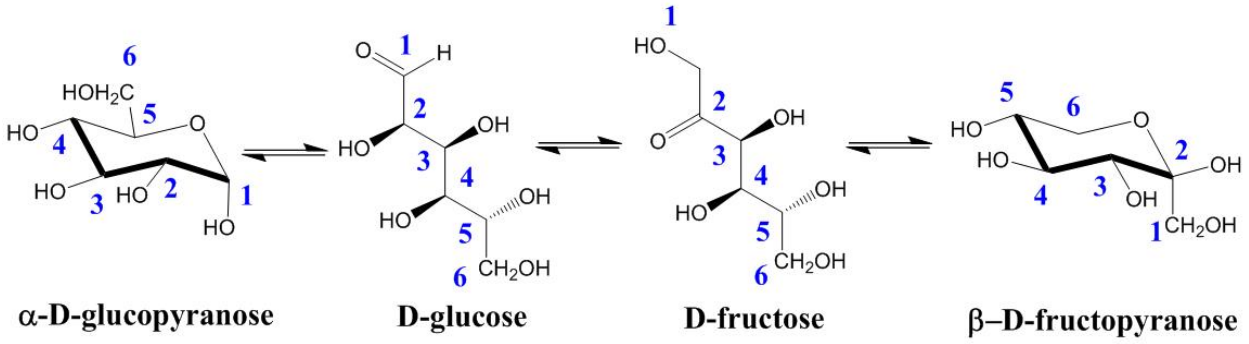

FIG. 5. Conversion of D-Glucose to D-Fructose by Interconversion. The complete reaction catalyzed by XI is believed to involve three major steps: (1) ring opening, (2) isomerization, and (3) ring closure.

Xylose Isomerase catalyzes the interconversion of D-Glucose to D-Fructose as shown in Fig. 5. Here, we are concerned with the isomerization (interconversion) step corresponding to linear glucose in the XI-Ni-LinearSugar_xn (3KCO) structure described by Kovalevski *et al.* [19] that provides proton locations. However, the 3KCO structure is a superposition of enzymes with Ni2A and Ni2B occupation (shown in Fig. 6A) that does not provide mechanistic details of the isomerization reaction. Previous theoretical work on XI has been

based on X-ray data, without knowledge of proton locations, and also with severely limited quantum regions [22, 32, 33] (i.e. not including shoe box rings, *etc*).

In this work, we have constructed a large, quantum only description of the active site by matching unperturbed (overlapping) atoms shared at the periphery by both 3KCO (linear sugar) and 3KCL (cyclic sugar) structures [19], with Mg substituted at the M1 and M2A positions. The model is charge neutral, involving 306 atoms including W16+20+137, H54+220, D245+255+257+287, K183+289, E181+217, Q256, T90+91, N92, F26+94, Mg391+392, GLO401 (glucose), & HOH1001+1095+1105+1106+1159+1190+1193+1163+1209. Hard constraints were imposed on 101 heavy atoms at the truncated, methylated periphery, and the interior including 9 water molecules and glucose was optimized (relaxed) at the B3LYP/6-31G** and B3LYP/6-311G** levels of theory [34, 35] to arrive at our initial state (Fig. 1A, Fig. 6B and Video 1). Our relaxation protocol involved fixing all interior heavy atoms first and relaxing protons, then relaxing waters and heavy atoms except those of the sugar, and finally full relaxation of all interior atoms. All calculations were carried out with version `beta:ad3a92337b33bef270e2288173fe3b804df07d54` of the linear scaling electronic structure code `FreeON` [36] using `tight` threshold levels and $\mathcal{O}(N)$ algorithms throughout, with gradients converged to within 0.2 ev/Å, corresponding to a precision of at least 2 significant digits in reported energy differences. Starting with **I**, structures **II** through **VII** were generated with simple constrained internal coordinate optimization [27] involving Mg2, glucose O2H and O1H, leading to structures **III**, **V** and **VII**. The intermediate, transition state structures **II**, **IV** and **VI** were obtained through linear synchronous transit followed by iteration with the climbing image version of the Nudged Elastic Band (NEB) [37], with movies of these reaction paths given in Video 2 (I→III), Video 3 (III→V) and Video 4 (V→VI). All calculations were carried out in serial with a variety of Intel and AMD 64 bit servers. Finally, the entire putative mechanism is outlined in Fig. 7.

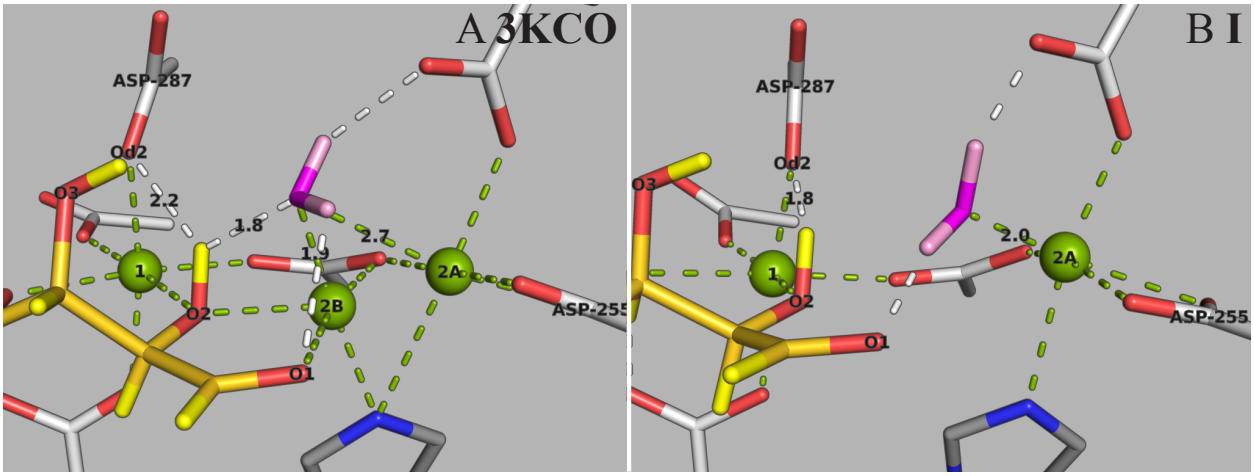

FIG. 6. The 3KCO active site with M1, M2A & M2B in green in A, and the relaxed model structure **I**.

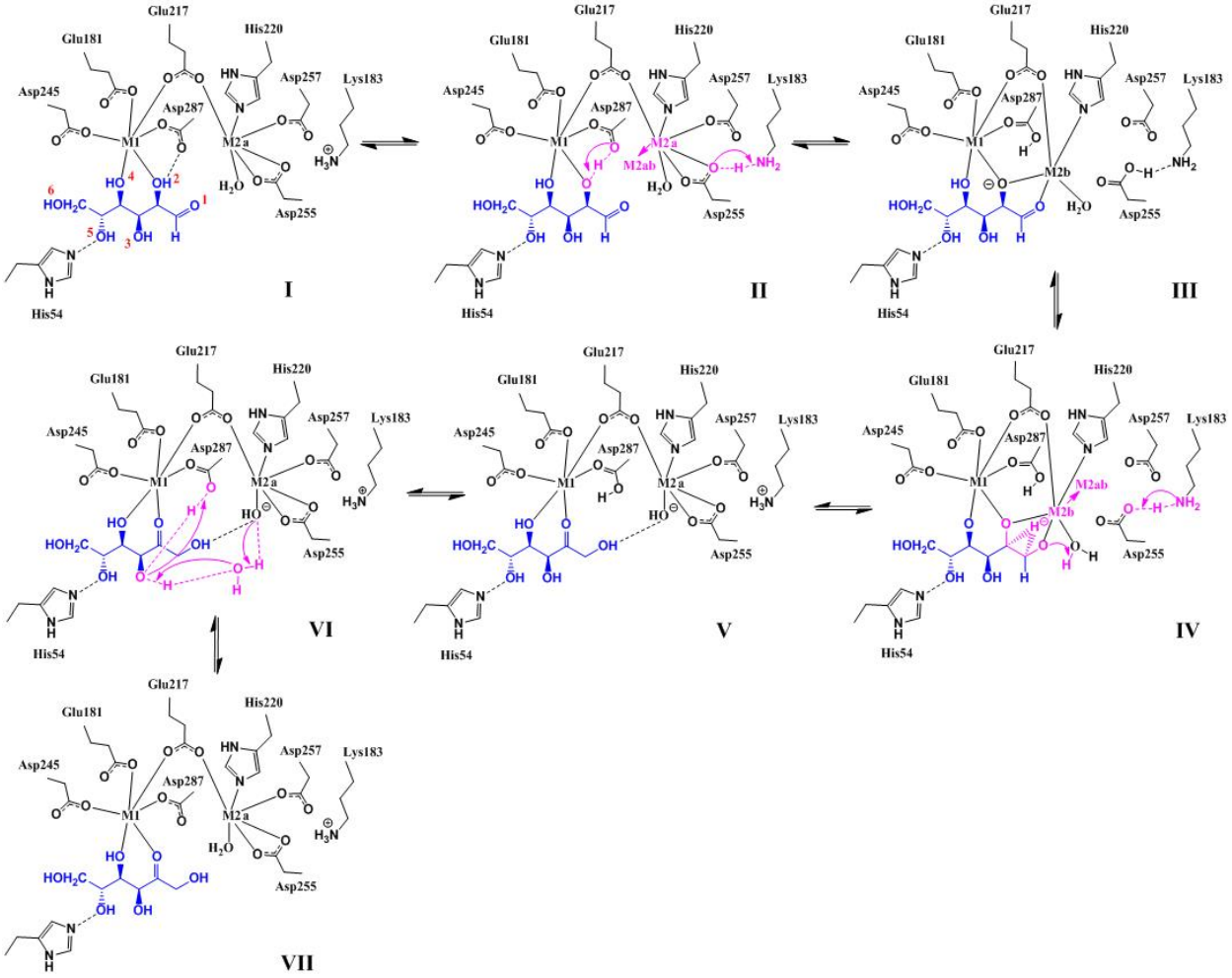

FIG. 7. Diagramatic respresentation of the proposed "hydroxide once" mechanism of D-glucose isomerization, cooresponding to structures **I-VII** in Figs.1-3, and the energy diagram in Fig.4.